

# Existence of the magnetization plateau in a class of exactly solvable Ising-Heisenberg chains

Jozef Strečka<sup>1</sup> and Michal Jašcur<sup>2</sup>

Department of Theoretical Physics and Astrophysics, Faculty of Science,

P. J. Šafárik University, Moyzesova 16, 041 54 Košice, Slovak Republic

E-mail addresses: jozkos@pobox.sk<sup>1</sup>, jascur@kosice.upjs.sk<sup>2</sup>

Submitted: June 7, 2021

## Abstract

The mapping transformation technique is applied to obtain exact results for the spin-1/2 and spin- $S$  ( $S = 1/2, 1$ ) Ising-Heisenberg antiferromagnetic chain in a presence of external magnetic field. Within this scheme, a field-induced first-order metamagnetic phase transition resulting in multiplateau magnetization curves, is investigated in detail. It is found that the scenario of the plateau formation depends fundamentally on the ratio between Ising and Heisenberg interaction parameters, as well as on the XXZ Heisenberg exchange anisotropy strength.

PACS:05.50.+q, 75.10.Jm, 75.10.Hk

*Keywords:* Ising-Heisenberg model; Exact solution; Quantum antiferromagnetism

## 1 Introduction

Quantum antiferromagnetism in lower dimensions is one of the most fascinating subjects in the condensed matter physics. In particular, the antiferromagnetic quantum Heisenberg chains (AFQHC) with small spins have attracted much attention on account of the rich quantum behaviour they display. Nevertheless, due to the strong quantum fluctuations the classical Néel state is not more an eigenstate of the Hamiltonian and thus, more interesting quantum phases should be expected to occur in the ground state. The nature of these phases, however, basically depends on the spin value of atoms. In fact, as conjectured Haldane [1] in 1983, the integer spin AFQHC have a finite energy gap between the ground state and the first excited state, while the half-odd integer ones possess a gapless excitation spectrum.

Another striking feature of the AFQHC is the appearance of fractional magnetization plateaus in the magnetization process. Extending the original Lieb-Schultz-Mattis theorem [2] Oshikawa, Yamanaka and Affleck (OYA) [3] argued that the magnetization per site  $m$  can be topologically quantized as:  $p(S_u - m) = \text{integer}$ , where  $p$  is a period of ground state in the thermodynamic limit and  $S_u$  denotes a total spin of an elementary

unit. However, this condition represents just the necessary condition for the plateau-state formation and does not directly prove its existence. It is therefore of interest to investigate how the plateau state is related to the periodicity of specific model [4]. Moreover, from the theoretical viewpoint the plateau state can also be regarded as a spin-gap state. Hence, the zero-temperature magnetization curves with plateaus bring an insight into the ground-state properties of the system, since the field-induced spin gaps reflect the gapped excitation spectrum.

Despite of an extensive theoretical effort focused on AFQHC, there still exist only few exactly solvable models with pure Heisenberg exchange interactions [5], especially for mixed-spin chains [6]. On the other hand, an exact solution for the chains with alternating Ising- and Heisenberg-type exchange interactions can be attained in less sophisticated manner. Indeed, the exact solution for the Ising-Heisenberg bond alternating chain (originally proposed and solved by Lieb *et al* [2]), has been recently successfully generalized to the case of anisotropic Heisenberg interaction [7]. In order to avoid mathematical complexities connected with the noncommutability of relevant spin operators, we will introduce in this article another class of the Ising-Heisenberg chains (with period  $p = 3$ ), that can be treated exactly within the mapping transformation method. However, the considered model naturally enables to analyse in detail the mutual competition between Ising- and Heisenberg-type interactions and moreover, it also proves to be very useful in view of the confirmation of multiplateau magnetization curves by an exact calculation.

This paper is organized as follows. In Sec. 2 the detailed description of the model, as well as the fundamental aspects of transformation technique are presented. In Sec. 3 we are concerned with the analysis of the most interesting numerical results for typical spin cases and finally, in Sec. 4 some concluding remarks are also drawn.

## 2 Model and method

In this article we will study a mixed spin-1/2 and spin- $S$  ( $S = 1/2, 1$ ) Ising-Heisenberg chain in a presence of external magnetic field. The structure of the considered mixed-spin chain is depicted in Fig.1, where the black circles denote the spin-1/2 atoms and the grey ones represent the spin- $S$  atoms. The total Hamiltonian of the system is given by:

$$\hat{\mathcal{H}} = J \sum_{i,j} [\Delta(\hat{S}_i^x \hat{S}_j^x + \hat{S}_i^y \hat{S}_j^y) + \hat{S}_i^z \hat{S}_j^z] + J_1 \sum_{k,l} \hat{S}_k^z \hat{\mu}_l^z - H_A \sum_l \hat{\mu}_l^z - H_B \sum_k \hat{S}_k^z, \quad (1)$$

where  $\hat{\mu}_l^z$  and  $\hat{S}_k^\alpha$  ( $\alpha = x, y, z$ ) denote the well-known components of standard spin-1/2 and spin- $S$  ( $S = 1/2, 1$ ) operators, respectively. The parameter  $J$  stands for the Heisenberg interaction between nearest-neighbouring spin- $S$  atoms (the grey atoms) and  $\Delta$  is the anisotropy parameter that allows to control the anisotropic XXZ interaction between an easy-axis regime ( $\Delta < 1$ ) and an easy-plane regime ( $\Delta > 1$ ). Furthermore, the interaction parameter  $J_1$  describes the Ising-type exchange interaction between pairs of nearest-neighbouring spin-1/2 and spin- $S$  atoms and finally, the terms incorporating  $H_A$  and  $H_B$  respectively, describe the coupling of spin-1/2 atoms and spin- $S$  atoms to an external magnetic field. As we can see from Fig.1, all pairs of nearest-neighbouring Heisenberg atoms are surrounded by Ising-type atoms only, thus the model under investigation can also be viewed as an Ising model the bonds of which are doubly decorated

by the Heisenberg atoms. In view of further manipulations, it is useful to rewrite the total Hamiltonian  $\hat{\mathcal{H}}$  as a sum of the bond Hamiltonians, i.e.  $\hat{\mathcal{H}} = \sum_{k=1}^N \hat{\mathcal{H}}_k$ , where  $N$  denotes the total number of Ising-type atoms and the summation runs over all bonds of the original (undecorated) chain. The bond Hamiltonian  $\hat{\mathcal{H}}_k$  contains all the interaction terms associated with the  $k$ th couple of Heisenberg atoms (see Fig.1), and it is given by

$$\begin{aligned} \hat{\mathcal{H}}_k = & J[\Delta(\hat{S}_{k1}^x \hat{S}_{k2}^x + \hat{S}_{k1}^y \hat{S}_{k2}^y) + \hat{S}_{k1}^z \hat{S}_{k2}^z] + J_1(\hat{S}_{k1}^z \hat{\mu}_{k1}^z + \hat{S}_{k2}^z \hat{\mu}_{k2}^z) \\ & - H_B(\hat{S}_{k1}^z + \hat{S}_{k2}^z) - H_A(\hat{\mu}_{k1}^z + \hat{\mu}_{k2}^z)/2. \end{aligned} \quad (2)$$

Now, exploiting the usual commutation relation for the bond Hamiltonians (i.e.  $[\hat{\mathcal{H}}_k, \hat{\mathcal{H}}_j] = 0$ , for  $k \neq j$ ), the partition function of the system can be partially factorized, namely,

$$\mathcal{Z} = \text{Tr}_{\{\mu\}} \prod_{k=1}^N \text{Tr}_{S_{k1}} \text{Tr}_{S_{k2}} \exp(-\beta \hat{\mathcal{H}}_k). \quad (3)$$

In above,  $\beta = (k_B T)^{-1}$ ,  $k_B$  being Boltzmann constant and  $T$  the absolute temperature.  $\text{Tr}_{\{\mu\}}$  means a trace over the degrees of freedom of the Ising spins and  $\text{Tr}_{S_{k1}} \text{Tr}_{S_{k2}}$  denotes a trace over the  $k$ th couple of Heisenberg spins. At this stage one easily observes that the structure of relation (3) implies a possibility to introduce the decoration-iteration mapping transformation [8]

$$\text{Tr}_{S_{k1}} \text{Tr}_{S_{k2}} \exp(-\beta \hat{\mathcal{H}}_k) = A \exp[\beta R \mu_{k1}^z \mu_{k2}^z + \beta H_0 (\mu_{k1}^z + \mu_{k2}^z)/2]. \quad (4)$$

As usual, the unknown transformation parameters  $A$ ,  $R$  and  $H_0$  can be attained by taking into account remaining degrees of freedom of both Ising spins ( $\mu_{k1}$  and  $\mu_{k2}$ ). In this way one obtains for the transformation parameters  $A$ ,  $R$  and  $H_0$  the following expressions

$$A = (V_1 V_2 V_3^2)^{1/4}, \quad \beta R = \ln\left(\frac{V_1 V_2}{V_3^2}\right), \quad \beta H_0 = \beta H_A - \ln\left(\frac{V_1}{V_2}\right), \quad (5)$$

where the functions  $V_1$ ,  $V_2$  and  $V_3$  depend on the spin value of Heisenberg atoms, as well as on the parameters of Hamiltonian (1) and they are summarized for both investigated spin cases in the Appendix.

Here, one should emphasize that the mapping relations (4)-(5) enable to transform the Ising-Heisenberg mixed-spin chain onto a simple spin-1/2 Ising chain with an effective exchange parameter  $R$ , placed in an external magnetic field of the magnitude  $H_0$ . Indeed, substituting (4) into (3) gives the following equality

$$\mathcal{Z}(\beta, J, J_1, \Delta, H_A, H_B) = A^N \mathcal{Z}_0(\beta, R, H_0), \quad (6)$$

which relates the partition function of Ising-Heisenberg chain  $\mathcal{Z}$  and that one of the spin-1/2 Ising chain  $\mathcal{Z}_0$ . Since the explicit expression for  $\mathcal{Z}_0$  is well known [9], we can then straightforwardly calculate all relevant thermodynamic quantities. For example, the Gibbs free energy  $\mathcal{G}$  of the mixed-spin Ising-Heisenberg chain is given by

$$\mathcal{G} = \mathcal{G}_0 - N k_B T \ln A, \quad (7)$$

where  $\mathcal{G}_0 = -k_B T \ln \mathcal{Z}_0$  denotes the Gibbs free energy of the corresponding spin-1/2 Ising chain. Next, by differentiating the Gibbs free energy  $\mathcal{G}$  with respect to  $H_A$  and

$H_B$  respectively, one directly obtains solution for the total sublattice magnetization. Of course, other thermodynamic quantities can also be calculated on the basis of familiar thermodynamic relations, e. g. the entropy  $S$  and the specific heat  $C$  can be calculated from

$$S = -\left(\frac{\partial G}{\partial T}\right)_H, \quad C = -T\left(\frac{\partial^2 G}{\partial T^2}\right)_H. \quad (8)$$

Nevertheless, a similar thermodynamic approach cannot be used for the calculation of other important quantities such as staggered magnetization, quadrupolar momentum or some correlations. Fortunately, Eq. (6) in conjunction with the transformation formula (4) allows after an elementary algebra the derivation of following exact spin identities [10]

$$\begin{aligned} \langle f_1(\hat{\mu}_i^z, \hat{\mu}_j^z, \dots \hat{\mu}_k^z) \rangle &= \langle f_1(\hat{\mu}_i^z, \hat{\mu}_j^z, \dots \hat{\mu}_k^z) \rangle_0, \\ \langle f_2(\hat{S}_{k1}^\alpha, \hat{S}_{k2}^\gamma, \hat{\mu}_{k1}^z, \hat{\mu}_{k2}^z) \rangle &= \left\langle \frac{\text{Tr}_{S_{k1}} \text{Tr}_{S_{k2}} f_2(\hat{S}_{k1}^\alpha, \hat{S}_{k2}^\gamma, \hat{\mu}_{k1}^z, \hat{\mu}_{k2}^z) \exp(-\beta \hat{\mathcal{H}}_k)}{\text{Tr}_{S_{k1}} \text{Tr}_{S_{k2}} \exp(-\beta \hat{\mathcal{H}}_k)} \right\rangle, \end{aligned} \quad (9)$$

with arbitrary function  $f_1$  depending exclusively on Ising spin variables and the function  $f_2$  depending on the spin variables from the  $k$ th bond only. The superscript  $\alpha, \gamma \equiv (x, y, z)$  label the spatial components of spin operators and finally, the symbols  $\langle \dots \rangle$  and  $\langle \dots \rangle_0$  stand for the standard ensemble average in the Ising-Heisenberg and its equivalent simple Ising model, respectively. However, the above spin identities considerably simplify the calculation of a large number of quantities. Indeed, for the reduced sublattice magnetization  $(m_A^z, m_B^z)$ , the total single-site magnetization  $m$  and the staggered sublattice magnetization  $(m_A^s, m_B^s)$ , one attains after straightforward algebra

$$\begin{aligned} m_A^z &\equiv \frac{1}{2} \langle \hat{\mu}_{k1}^z + \hat{\mu}_{k2}^z \rangle = \frac{1}{2} \langle \hat{\mu}_{k1}^z + \hat{\mu}_{k2}^z \rangle_0 \equiv m_0, \\ m_B^z &\equiv \frac{1}{2} \langle \hat{S}_{k1}^z + \hat{S}_{k2}^z \rangle = (V_4/V_1 - V_5/V_2 + 2V_6/V_3)/2 \\ &\quad - 2m_0(V_4/V_1 + V_5/V_2) + 2\varepsilon_0(V_4/V_1 - V_5/V_2 - 2V_6/V_3), \\ m &\equiv (m_A^z + 2m_B^z)/3, \\ m_A^s &\equiv \frac{1}{2} \langle \hat{\mu}_{k1}^z - \hat{\mu}_{k2}^z \rangle = \frac{1}{2} \langle \hat{\mu}_{k1}^z - \hat{\mu}_{k2}^z \rangle_0 \equiv m_0^s, \\ m_B^s &\equiv \frac{1}{2} \langle \hat{S}_{k1}^z - \hat{S}_{k2}^z \rangle = -m_0^s V_7/V_3. \end{aligned} \quad (10)$$

In above,  $m_0$ ,  $m_0^s$  and  $\varepsilon_0$  represent the reduced magnetization, staggered magnetization and nearest-neighbour correlation of the corresponding undecorated Ising chain and the coefficients  $V_1$ - $V_7$  are listed for both investigated spin cases in the Appendix.

Finally, let us define some pair correlation functions and the quadrupolar momentum, which are also very useful for understanding of magnetic properties of the system, namely,

$$\begin{aligned} q_{hh}^{xx} &\equiv \langle \hat{S}_{k1}^x \hat{S}_{k2}^x \rangle \equiv \langle \hat{S}_{k1}^y \hat{S}_{k2}^y \rangle, & q_{hh}^{zz} &\equiv \langle \hat{S}_{k1}^z \hat{S}_{k2}^z \rangle, & q_{ii}^{zz} &\equiv \langle \hat{\mu}_{k1}^z \hat{\mu}_{k2}^z \rangle \equiv \varepsilon_0, \\ q_{ih}^{zz} &\equiv \frac{1}{2} \langle \hat{S}_{k1}^z \hat{\mu}_{k1}^z + \hat{S}_{k2}^z \hat{\mu}_{k2}^z \rangle, & \eta &\equiv \frac{1}{2} \langle (\hat{S}_{k1}^z)^2 + (\hat{S}_{k2}^z)^2 \rangle. \end{aligned} \quad (11)$$

In these equations, the subscripts denote the type of atoms and superscripts the space direction. One should also notice that the definition of the parameter  $\eta$  is obviously

meaningful for  $S \geq 1$  only. Although, the derivation of relevant equations for these quantities is straightforward, the calculation procedure by itself is rather lengthy and tedious, thus the details are not presented here.

### 3 Numerical results and discussion

Before discussing the most interesting numerical results, it is worth mentioning that some preliminary results for the ferromagnetic version of the model ( $J < 0, J_1 < 0$ ) have already been published by the present authors elsewhere [11]. For this reason, in this article we will restrict our attention to the doubly decorated Ising-Heisenberg chain with antiferromagnetic interactions only (i.e.  $J > 0, J_1 > 0$ ). The particular attention is focused on the ground-state analysis and the appearance of plateaus in the chains with different decorating spin  $S$ . Among other matters, we will directly prove the existence of double-plateau magnetization curve in the spin  $S = 1/2$  chain, more precisely, the magnetization curve with plateaus at  $m = 0$  and  $1/6$ . On the other hand, in the spin  $S = 1$  chain a greater diversity of magnetization process will be confirmed, in fact, we will prove the existence of double-plateau ( $m = 0$  and  $1/2$ ), triple-plateau ( $m = 0, 1/6$  and  $1/2$ ) and quadruple-plateau ( $m = 0, 1/6, 1/3$  and  $1/2$ ) magnetization curves.

In addition, since each couple of the Heisenberg atoms is surrounded by the Ising atoms only, the relevant spin deviations cannot propagate through the Ising bonds and therefore, the quantum fluctuations are necessarily localized within the unit cell (within the four-spin cluster consisting of the Heisenberg spin pair and its nearest-neighbouring Ising spins). Owing to this fact, the observed plateaus cannot be considered as the OYA plateaus, i. e. the plateaus with collective eigenstate extending over the whole chain. Nevertheless, it is interesting to note that all observed fractional magnetization satisfy the OYA condition for  $p = 6$  (the period of translational symmetry should be twice as large as the periodicity of Hamiltonian as a consequence of an antiferromagnetic nature of ground state).

#### 3.1 Spin $S = 1/2$ chain

We begin our analysis by considering the effect of exchange anisotropy  $\Delta$  and uniform magnetic field (i.e.  $H_A = H_B = H$ ) on the ground-state phase boundaries of the spin  $S = 1/2$  chain. For this purpose, we have displayed in Fig.2 some typical ground-state phase diagrams in the  $\Delta - H/J$  plane for  $J_1/J = 1.0$  and  $2.0$ . As one can see from this figure, the relevant phase boundaries separate three or four distinct phases, namely, the antiferromagnetic (AF), ferrimagnetic I (FI), ferrimagnetic II (FII) and saturated paramagnetic (SP) phase. One also observes that both ferrimagnetic phases (FI and FII) represent an intermediate phase between AF and SP phase occurring due to the first-order metamagnetic transition. As we have already mentioned before, different phases can be distinguished by analysing the magnetization and the correlation functions at  $T = 0$ . In this way one finds the following ground-state results for particular phases:

Antiferromagnetic phase (AF):

$$(q_{hh}^{xx}, q_{hh}^{zz}, q_{ih}^{zz}, q_{ii}^{zz}, m_A^s, m_B^s) = (-J\Delta Q^{-1}, -1/4, -J_1 Q^{-1}, -1/4, 1/2, -2J_1 Q^{-1});$$

where we have defined the function  $Q = 4\sqrt{J_1^2 + (J\Delta)^2}$ , in order to write the relevant expressions in more abbreviated and elegant form.

Ferrimagnetic phase I (FI):

$$(q_{hh}^{xx}, q_{hh}^{zz}, q_{ih}^{zz}, q_{ii}^{zz}, m_A^z, m_B^z, m) = (-1/4, -1/4, 0, 1/4, 1/2, 0, 1/6);$$

Ferrimagnetic phase II (FII):

$$(q_{hh}^{xx}, q_{hh}^{zz}, q_{ih}^{zz}, q_{ii}^{zz}, m_A^z, m_B^z, m) = (0, 1/4, -1/4, 1/4, -1/2, 1/2, 1/6);$$

Saturated paramagnetic phase (SP):

$$(q_{hh}^{xx}, q_{hh}^{zz}, q_{ih}^{zz}, q_{ii}^{zz}, m_A^z, m_B^z, m) = (0, 1/4, 1/4, 1/4, 1/2, 1/2, 1/2).$$

Moreover, it is also noteworthy that all ground-state phase boundaries can be expressed analytically as follows (see Fig.2),

a) for  $J_1/J \leq 1.0$

$$(1) H/J = \sqrt{\Delta^2 + (J_1/J)^2} - \Delta, \quad (2) H/J = (\Delta + J_1/J)/2 + 1/2, \quad (12)$$

b)  $J_1/J > 1.0$

$$(1) H/J = \sqrt{\Delta^2 + (J_1/J)^2} - \Delta, \quad (2) H/J = (\Delta + J_1/J)/2 + 1/2, \quad (13)$$

$$(3) H/J = \sqrt{\Delta^2 + (J_1/J)^2} - J_1/J + 1, \quad (4) H/J = J_1/J, \quad (5) \Delta = J_1/J - 1.$$

In order to demonstrate the diversity of the magnetization process, we have plotted in Fig.3 the low-temperature magnetization curves for various exchange anisotropies  $\Delta$ . The detailed examination of these dependencies reveals that the mechanism of the magnetization process depends basically on the ratio between Ising and Heisenberg interaction constants, more specifically, on whether  $J_1/J \leq 1.0$  or  $J_1/J > 1.0$ . In the former case, the plateau state arises due to the alignment of the Ising spins towards the external-field direction (FI phase) regardless of the anisotropy strength  $\Delta$  (see Fig.3a). Naturally, in this case there is no other possibility for the formation of intermediate plateau. On the other hand, in the case of  $J_1/J > 1.0$  the metamagnetic transition to the FI phase can be observed for the stronger anisotropies  $\Delta$  only (see Fig.3d), while for the weaker anisotropies the FII phase becomes the stable one. In this phase, the Heisenberg (Ising) spins align parallel (antiparallel) with respect to the external-field direction as it is apparent from Fig.3b. Moreover, the situation for the most interesting point at which both intermediate phases (FI and FII) coexist, is depicted in Fig.3c. Referring to this plot, the coexistence of both ferrimagnetic phases is also reflected in the mixed feature of the magnetization curve (compare magnetization curve from Fig.3c with those in Figs.3b and 3d).

In order to enable an independent check of the magnetization scenario, we have also studied the relevant low-temperature dependencies of the nearest-neighbour correlation functions introduced in Eq. (11). In Fig.4a, the variations of the correlation functions with anisotropy  $\Delta$  are shown for the system without external magnetic field. As one can see, the correlation function  $q_{hh}^{zz}$  between Heisenberg spins takes its saturation value irrespectively of  $\Delta$ , what means that all nearest-neighbouring Heisenberg spin pairs align antiparallel with respect to each other. Moreover, the saturated value of correlation

$q_{ii}^{zz} = -1/4$  indicates a perfect antiferromagnetic alignment also in the Ising sublattice (between third nearest-neighbour Ising spins). Contrary to this behaviour, the perfect antiparallel alignment between Ising and Heisenberg spins is destroyed as  $\Delta$  increases from zero (see the correlation  $q_{ih}^{zz}$ ). Hence, the Ising and Heisenberg spins are oriented randomly with respect to each other, the degree of randomness being the greater, the stronger the exchange anisotropy  $\Delta$ . In addition, it is clear that the anisotropy term  $\Delta$  is also responsible for the onset of an interesting short-range ordering (nonzero  $q_{hh}^{xx}$ ) in  $xy$  plane. Anyway, the value of correlation  $q_{hh}^{xx}$  can be thought as a measure of the strength of local quantum fluctuations appearing in the spin system. Furthermore, in Figs.4b-4d we have displayed the field dependencies of the correlation functions corresponding to the magnetization curves from Figs.3b-3d. The depicted behaviour for the correlation functions is in complete agreement with results for the magnetization curves and moreover, it enables better understanding of the magnetic ordering in relevant phases. As a typical example we can mention the ferrimagnetic phases. Although the total magnetization of both the FI and FII phases is the same, the results for other quantities indicate a fundamental difference between them. In fact, in the FI phase the pairs of Heisenberg spins create singlet dimers and thus, they do not contribute to the total magnetization which is nonzero due to the fully polarized Ising spins only, as already stated before. This observation would suggest that the formation of FI plateau state should be based on the quantum mechanism with a significant influence of local quantum fluctuations. In contrast to this, the FII phase represents the standard ferrimagnetically ordered phase usually observed in the pure Ising systems. Indeed, the generation of the FII plateau state is nothing but the gapped excitation from the Néel state, implying the magnetization process with a 'classical' Ising-like mechanism. Finally, one should notice that after exceeding the saturation field given by conditions (12) and (13), the ground state becomes fully polarized (SP phase) and all spins are aligned in the external-field direction.

Now, let us investigate the finite-temperature behaviour of the system. Firstly, we take a closer look at the thermal dependencies of total magnetization that are shown in Fig.5. As one can see, the initial value of total magnetization takes one of three possible values  $m = 0, 1/6$  or  $1/2$  for the AF, FI (FII) or SP phase, respectively. Furthermore, there are two special cases which correspond to the coexistence of the relevant phases. In these cases, we have obviously obtained  $m = 1/12$  or  $1/3$  at  $T = 0$ . It is also easy to observe here that the most interesting dependencies appear for external fields from the neighbourhood of phase boundaries. Hence, the observed rapid increase (decrease) of the magnetization can be attributed to the thermal excitations of huge number of spins which occur due to the competitive influence of both phases.

For completeness, we have also plotted the entropy (Fig.6a) and the specific heat (Fig.6b-6d) as a function of temperature. As one can expect, the entropy of the system does not vanish for the boundary external-field values  $H/J = 1.0$  and  $2.25$ , at which the relevant phases coexist in the ground state (see Fig.6a). However, we should mention that for any other external fields the entropy vanishes as the temperature goes to zero. Another quantity which is interesting also from the experimental point of view represents the specific heat. The thermal variations of this quantity are depicted in Fig.6b for the same values of  $H/J$  as for entropy in Fig.6a. The displayed behaviour indicates a round Schottky-type maximum, whereas the stronger the external field, the flatter and

the broader the maximum. Apart from this trivial finding, one can also observe the double-peak specific heat curves (see Figs.6c and 6d). The first peak which occurs in the specific heat curve at lower temperature is evidently closely related to the rapid variation of the magnetization (compare Fig.6c-d with Fig.5b). Moreover, it turns out that the maximum of this peak can be located approximately in the middle of ferrimagnetic region (in our case around  $H/J \approx 1.5$ ). On the other hand, the second peak may be thought as a Schottky-like peak resulting from the antiferromagnetic short-range order. Indeed, the relevant thermal dependencies for the nearest-neighbouring correlations strongly support this statement.

In the following subsection we examine the spin  $S = 1$  chain in order to clarify the influence of decorating spin on the magnetic properties of the system.

### 3.2 Spin $S = 1$ chain

We start our discussion once again with the analysis of ground state. In order to establish correct ground-state phase boundaries all relevant quantities have been examined in detail. From this analysis one can conclude that depending on the ratio between  $J_1$ ,  $J(\Delta)$  and  $H$ , altogether six different phases can appear in the ground state (see ground-state phase diagrams in Figs.7a and 9a-b). In this part, we will firstly describe details of the spin ordering emerging in the appropriate ground-state phases and then, we will show how the scenario of the magnetization process depends on the parameters of the model.

In the antiferromagnetic phase (AF) one finds a perfect antiferromagnetic alignment in the Ising sublattice (i.e.  $m_A^s = 1/2$  and  $q_{ii}^{zz} = -1/4$ ) regardless of the strength of the exchange anisotropy  $\Delta$ . Accordingly, the relevant spin order in the Ising sublattice is completely identical to that one in the AF phase of the spin  $S = 1/2$  chain. Nevertheless, in contrast to the spin  $S = 1/2$  case, the antiparallel alignment between nearest-neighbouring Heisenberg spins is weakened along  $z$ -axis as  $\Delta$  increases from zero. In fact, the correlation  $q_{hh}^{zz}$  tends monotonically from its classical Ising value  $q_{hh}^{zz} = -1$  at  $\Delta = 0$  to  $q_{hh}^{zz} = -1/2$  for large  $\Delta$  (see e. g. Fig.8a). In addition, one easily proves also the validity of relation  $\eta = |q_{hh}^{zz}|$  in the whole AF region. This observation would suggest that  $\Delta$  supports the spin reorientation of Heisenberg spin pairs, namely, from the antiparallel oriented Heisenberg spin pair (one spin in  $S^z = -1$  state, another one in spin  $S^z = 1$  state to be further denoted as the '1 - 1' spin pair) towards the spin pair with both Heisenberg spins in the spin  $S^z = 0$  state (the '00' spin pair). However, in the large  $\Delta$  limit both types of the Heisenberg spin pairs ('1 - 1' as well '00') are equally well populated and with a high probability also randomly distributed among Ising spins. This suggestion is strongly supported by results for the correlation  $q_{ih}^{zz}$  and staggered magnetization  $m_B^s$  which asymptotically tend to zero as  $\Delta \rightarrow \infty$  (Fig.8a). Finally, one should also notice that all these effects could originate from the onset of the antiferromagnetic short-range-ordering in the  $xy$  plane (nonzero  $q_{hh}^{xx}$ ) that is the stronger (up to the value  $1/\sqrt{2}$ ), the greater the exchange anisotropy strength  $\Delta$ .

Now, let us turn our attention to both the FI and FII ferrimagnetic phases. As in the spin  $S = 1/2$  case, the nonzero total magnetization of the FI phase arises due to the fully polarized Ising spins only ( $m_A^z = 1/2$  and  $q_{ii}^{zz} = 1/4$ ), while the Heisenberg sublattice does not contribute to the total magnetization at all ( $m_B^z = 0$  and  $q_{ih}^{zz} = 0$ ). Since the FI



phase can arise by increasing the external field from the AF phase only (see Fig.7a, 9ab), it is of interest to compare the relevant spin ordering in both phases. Actually, one still finds  $\eta = |q_{hh}^{zz}|$  to be valid, however, the nearest-neighbour correlation  $q_{hh}^{zz}(q_{hh}^{xx})$  is weaker (stronger) in the FI phase with respect to that one in the AF phase (Fig.8d). These results are taken to mean that the number of nearest-neighbouring '00' spin pairs increases (of course, only up to one half of the total number of pairs) as one passes through the AF-FI phase boundary. Moreover, the appearance of a massive short-range order in the  $xy$  plane strongly implies the relevance of local quantum fluctuations also in the FI phase. On the other hand, in the second ferrimagnetic phase FII we have found the following results

$$(q_{hh}^{xx}, q_{hh}^{zz}, q_{ih}^{zz}, q_{ii}^{zz}, \eta, m_A^z, m_B^z, m) = (0, 1, -1/2, 1/4, 1, -1/2, 1, 1/2),$$

indicating the 'classical' character of this phase that is usually observed also in the pure Ising spin systems. As the relevant spin-ordering is thoroughly analogous to that one in the FII phase of spin  $S = 1/2$  chain, for brevity we will not repeat its description here.

The most interesting spin order, however, can be found in the valence-bond phase (VB) and the intermediate phase (IP). Really, for instance in the VB phase one finds

$$(q_{hh}^{xx}, q_{hh}^{zz}, q_{ih}^{zz}, q_{ii}^{zz}, \eta, m_A^z, m_B^z, m) = (-1/2, 0, 1/4, 1/4, 1/2, 1/2, 1/2, 1/2).$$

As one can see, in contrast to the fully polarized Ising sublattice ( $m_A^z = 1/2$  and  $q_{ii}^{zz} = 1/4$ ), each couple of the nearest-neighbouring Heisenberg spins consists of one polarized spin ( $S^z = 1$ ) and one spin in the  $S^z = 0$  state, i. e. the spin '01' pair. It is interesting to note that the symmetrization of both Heisenberg spin states can be achieved using the valence-bond-solid (VBS) picture [12]. Accordingly, each spin-1 atom splits into one polarized spin-1/2 variable with the fixed projection into the external field direction and one spin-1/2 variable with the unfixed projection creating a valence-bond. Thus, it is reasonable to assume that both Heisenberg spins interchange their spin states (tunneling between the  $S^z = 0$  and  $S^z = 1$  spin states) and therefore, they effectively act on the surrounding Ising spins as the spin-1/2 atoms (see also the result for correlation  $q_{ih}^{zz}$ ). However, the antiferromagnetic short-range order in the  $xy$  plane (nonzero  $q_{hh}^{xx}$ ), as well as the fact that the VB phase cannot be detected in the pure Ising system (i.e. for  $\Delta = 0$ ), imply again the obvious influence of the local quantum fluctuations.

Perhaps the most striking spin alignment has been discovered in the IP phase. Among other matters, the perfect antiferromagnetic alignment between the Ising spins ( $m_A^s = 1/2$  and  $q_{ii}^{zz} = -1/4$ ) has been confirmed in IP phase, hence, the total magnetization of system ( $m = 1/3$ ) is entirely determined by the contribution of Heisenberg spins. Anyway, the results for the Heisenberg sublattice magnetization  $m_B^z = 1/2$ , correlation function  $q_{hh}^{zz} = 0$  and quadrupolar momentum  $\eta = 1/2$ , clearly indicate that each couple of the nearest-neighbouring Heisenberg atoms comprises of the spin '01' pair. However, since both Heisenberg spins are placed in the IP phase between two non-equivalent Ising spins (one 'up', other 'down'), the spin state interchange between both Heisenberg atoms would lead to  $q_{ih}^{zz} = 0$  what is in contradiction with our numerical result  $q_{ih}^{zz} \neq 0$ . On the other hand, if the Heisenberg atom in spin  $S^z = 1$  state would be strictly antiferromagnetically coupled to its nearest-neighbouring Ising spin (spin 'down'), then we would have  $q_{ih}^{zz} = -1/4$ . Nevertheless, our result for the correlation  $|q_{ih}^{zz}| \ll 1/4$  indicates only the partial antiferromagnetic order between Ising and Heisenberg spins. This observation would

suggest that the spin '01' Heisenberg pairs should be, to a certain degree, randomly distributed among Ising spins. Finally, as one can expect, in the high field limit the system undergoes a phase transition towards the fully saturated paramagnetic phase (SP). As before, in the SP phase all Ising and Heisenberg spins are completely aligned towards the external-field direction, thus, in the SP phase one attains

$$(q_{hh}^{xx}, q_{hh}^{zz}, q_{ih}^{zz}, q_{ii}^{zz}, \eta, m_A^z, m_B^z, m) = (0, 1, 1/2, 1/4, 1, 1/2, 1, 5/6);$$

Now, let us proceed to examine the magnetization process of the system under investigation. For this purpose, we have shown in Figs.7a and 9a-b the ground-state phase diagrams in the  $\Delta - H/J$  plane together with some typical examples of the magnetization curves (Figs.7b-d and 9c-d) for three selected values of interaction parameters  $J_1/J$ . In order to provide an independent check of the magnetization scenario from Figs.7b-d, the corresponding field-dependencies of the correlation functions and quadrupolar momentum are displayed in Figs.8b-d. Obviously, all the above results are absolutely in accordance with the aforementioned ground-state spin ordering. Moreover, through the comparison of Figs.7a and 9a-b one can realize that the nature of magnetization process depends basically on the ratio between the Ising and Heisenberg interaction parameters. In fact, the stronger the Ising interaction  $J_1$  with respect to the Heisenberg one  $J(\Delta)$ , the broader the parameter region corresponding to the 'classical' FII phase. Otherwise, the increasing influence of the Heisenberg interaction  $J(\Delta)$  causes the broadening of regions corresponding to the FI and VB phase, respectively, until the FII phase completely vanishes below  $J_1/J < 2/3$ , see e. g. Fig.9a where the FII phase is already missing. Consequently, in the FI and VB phases one can expect that the effect of local quantum fluctuations plays an important role.

Although, the system exhibits a stepwise magnetization curve with an abrupt change of the magnetization in the whole range of parameters (see Figs.7b-d and 9c-d), there is a fundamental difference between the magnetization process in the 'classical' Ising-like regime and that one in the quantum regime. As a matter of fact, in the former case one observes the double-plateau magnetization curve with the FII plateau state only, i. e. with the FII phase as an intermediate state between the AF and SP phase (see Fig.7b). Contrary to this, in the latter case one can detect the double- (Fig.7c), triple- (Fig.7d), or quadruple-plateau (Fig.9c-d) magnetization curves. The double-plateau magnetization curves are rather rarely observable, since they arise due to the direct metamagnetic transition from the AF phase to the VB phase in a relatively narrow region of  $\Delta$  only (see Fig.7a). However, when the mechanism of the magnetization process is driven by the Heisenberg interaction, i. e. under the requirement of sufficiently small  $J_1/J$  and sufficiently large  $\Delta$ , the triple-plateau magnetization curves with the transitions between AF-FI-VB-SP phases are always preferred (Fig.7d). Finally, one should also remark that if the condition  $\Delta \approx H/J \approx J_1/J > 1$  is satisfied, there also appear the extraordinary quadruple-plateau magnetization curves (see Fig.9b) with the IP phase in a very narrow region of the external fields. Indeed, we found even two different possibilities for the quadruple-cascade transitions, namely, the AF-FI-IP-FII-SP cascade transitions (Fig.9c) as well as the AF-FI-IP-VB-SP ones (Fig.9d).

To conclude the analysis of the spin  $S = 1$  chain, we will also briefly mention the finite-temperature behaviour of the system under consideration. For this purpose, the

thermal variations of the total magnetization are plotted in Fig.10 for  $J_1/J = 1.0$  and two selected values of the anisotropy  $\Delta$ . In agreement with the aforementioned arguments, one observes here three and two field-induced transitions for the anisotropy strengths  $\Delta = 1.0$  and  $0.55$ , respectively. Evidently, as the magnitude of external field varies, the various thermal dependencies result from the competition between the Ising interaction, Heisenberg interaction and magnetic field. However, the most interesting dependencies arise again for the external fields from the vicinity of the phase boundaries. In such a case, the relevant thermal excitations result in a very rapid change of magnetization due to the competing influence of the phases separated by relevant transition line. Moreover, it turns out that the narrower interval of external fields corresponds to the relevant phase, the more robust change in the magnetization can be observed.

## 4 Conclusion

In the present article we have obtained the exact solution of the mixed spin-1/2 and spin- $S$  ( $S = 1/2, 1$ ) Ising-Heisenberg chain in the external magnetic field. The most important result stemming from this study is the confirmation of multistep magnetization process by an exact calculation. Moreover, it has been proved that the character of magnetization process depends essentially on the ratio between the Ising and Heisenberg interactions, whereas the XXZ anisotropy term  $\Delta$  also allows to control it in deciding manner. Since the presence of the non-diagonal interaction term  $J\Delta$  is responsible for the onset of the local quantum fluctuations, as we have also shown, it basically modifies an otherwise trivial Ising-like behaviour. For example, in the case of the spin  $S = 1$  chain one finds instead of the double-plateau magnetization curve arising in the pure Ising spin system ( $\Delta = 0$ ), the double-, triple-, or even quadruple-plateau magnetization curves in the Ising-Heisenberg chain with  $\Delta \neq 0$ . Altogether, the presented results indicate that the extraordinary rich ground-state phase diagrams result from the competition between the easy-axis interactions  $J_1, J$  and the easy-plane interaction  $J\Delta$ .

One should also emphasize that our research on Ising-Heisenberg chains has been stimulated by the recent experimental works dealing with many quasi-1D mixed-spin chains [13]. Although, we are not aware of any quasi-1D system in that two kinds of magnetic ions regularly alternate with  $p = 3$  periodic fashion (AABAAB...), the recent progress in molecular engineering [14] supports our hope that the synthesis of such a polymeric chain should be possible in the near future. Structural derivatives of a novel polymeric chain recently reported by Mukherjee *et al* [15], seem to be the most promising candidates from this point of view. In fact, the crystal structure of the above mentioned polymeric chain consists of the spin-1/2  $\text{Cu}^{\text{II}}$  dimers linked through  $\text{Ni}^{\text{II}}$  monomers. Unfortunately, as a consequence of the square-planar coordination of  $\text{Ni}^{\text{II}}$  ions in  $[\text{Ni}^{\text{II}}(\text{CN})_4]^{2-}$  bridging groups, the  $\text{Ni}^{\text{II}}$  metal ions are diamagnetic and thus, they do not contribute to the magnetism.

Finally, it should be stressed that the applied mapping transformation technique does not require any restriction to the dimensionality of the spin system and hence, it can be straightforwardly generalized to the mixed Ising-Heisenberg lattices in two- and three-dimensions, too [10].

*Acknowledgement:* The authors would like to thank referee for useful comments.  
This work was supported by the VEGA grant No. 1/9034/02 and APVT grant No. 20-009902.

## 5 Appendix

Explicit expressions for the functions  $V_1$ - $V_6$ .

a) Spin-1/2 chain:

$$\begin{aligned}
V_1 &= 2 \exp(-\beta J/4) \cosh(\beta J_1/2 + \beta H_B) + 2 \exp(\beta J/4) \cosh(\beta J\Delta/2) \\
V_2 &= 2 \exp(-\beta J/4) \cosh(\beta J_1/2 - \beta H_B) + 2 \exp(\beta J/4) \cosh(\beta J\Delta/2) \\
V_3 &= 2 \exp(-\beta J/4) \cosh(\beta H_B) + 2 \exp(\beta J/4) \cosh\left(\beta \sqrt{J_1^2 + (J\Delta)^2/2}\right) \\
V_4 &= \exp(-\beta J/4) \sinh(\beta J_1/2 + \beta H_B)/2 \\
V_5 &= \exp(-\beta J/4) \sinh(\beta J_1/2 - \beta H_B)/2 \\
V_6 &= \exp(-\beta J/4) \sinh(\beta H_B)/2, \\
V_7 &= \frac{2J_1 \exp(\beta J/4)}{\sqrt{J_1^2 + (J\Delta)^2}} \sinh\left(\beta \sqrt{J_1^2 + (J\Delta)^2/2}\right).
\end{aligned}$$

b) Spin-1 chain:

$$\begin{aligned}
V_1 &= 2 \exp(-\beta J) \cosh(\beta J_1 + 2\beta H_B) + \exp(2\beta J/3)W_1 + \\
&\quad + 4 \cosh(\beta J_1/2 + \beta H_B) \cosh(\beta J\Delta) \\
V_2 &= 2 \exp(-\beta J) \cosh(\beta J_1 - 2\beta H_B) + \exp(2\beta J/3)W_1 + \\
&\quad + 4 \cosh(\beta J_1/2 - \beta H_B) \cosh(\beta J\Delta) \\
V_3 &= 2 \exp(-\beta J) \cosh(2\beta H_B) + \exp(2\beta J/3)W_2 + \\
&\quad + 4 \cosh(\beta H_B) \cosh\left(\beta \sqrt{J_1^2 + (2J\Delta)^2/2}\right) \\
V_4 &= \exp(-\beta J) \sinh(\beta J_1 + 2\beta H_B) + \sinh(\beta J_1/2 + \beta H_B) \cosh(\beta J\Delta) \\
V_5 &= \exp(-\beta J) \sinh(\beta J_1 - 2\beta H_B) + \sinh(\beta J_1/2 - \beta H_B) \cosh(\beta J\Delta) \\
V_6 &= \exp(-\beta J) \sinh(2\beta H_B) + \sinh(\beta H_B) \cosh\left(\beta \sqrt{J_1^2 + (2J\Delta)^2/2}\right)
\end{aligned}$$

where the expressions  $W_1$  and  $W_2$  are given by:

$$\begin{aligned}
W_1 &= \sum_{n=0}^2 \exp\left\{-2\beta P_1 \cos[(\phi_1 + 2\pi n)/3]\right\}, \\
W_2 &= \sum_{n=0}^2 \exp\left\{-2\beta P_2 \cos[(\phi_2 + 2\pi n)/3]\right\}, \\
P_1^2 &= (J/3)^2 + 2(J\Delta)^2/3, & P_2^2 &= (J/3)^2 + 2(J\Delta)^2/3 + J_1^2/3, \\
Q_1 &= (J/3)^3 + J(J\Delta)^2/3, & Q_2 &= (J/3)^3 + J(J\Delta)^2/3 - J_1^3, \\
\phi_1 &= \arctan\left(\sqrt{P_1^6 - Q_1^2}/Q_1\right), & \phi_2 &= \arctan\left(\sqrt{P_2^6 - Q_2^2}/Q_2\right).
\end{aligned}$$

## References

- [1] Haldane F D M 1983 *Phys. Lett. A* **93** 464;  
Haldane F D M 1983 *Phys. Rev. Lett.* **50** 1153
- [2] Lieb E H, Schultz T D and Mattis D C 1961 *Ann. Phys. (N. Y.)* **16** 407;  
Lieb E H and Mattis D C 1962 *J. Math. Phys.* **3** 749
- [3] Oshikawa M, Yamanaka M and Affleck I 1997 *Phys. Rev. Lett.* **78** 1984;  
Affleck I 1998 *Phys. Rev. B* **37** 5186
- [4] Hida K 1994 *J. Phys. Soc. Jpn.* **63** 2359;  
Okamoto K 1995 *Solid State Commun.* **98** 245;  
Tonegawa T, Nakao T and Kaburagi H 1996 *J. Phys. Soc. Jpn.* **65** 3317;  
Pati S K, Ramasecha S and Sen D 1997 *Phys. Rev. B* **55** 8894;  
Sakai T and Takahashi M 1998 *Phys. Rev. B* **57** R3201;  
Totsuka K 1997 *Phys. Lett. A* **228** 103;  
Totsuka K 1998 *Phys. Rev. B* **57** 3454;  
Sakai T and Yamamoto S 1999 *Phys. Rev. B* **60** 4053;  
Yamamoto S and Sakai T 2000 *Phys. Rev. B* **62** 3795;  
Okamoto K and Kitazawa A 1999 *J. Phys. A: Math. Gen.* **32** 4601;  
Kitazawa A and Okamoto K 1999 *J. Phys.: Condens. Matter* **11** 9765;  
Koga A, Okunishi K and Kawakami N 2000 *Phys. Rev. B* **62** 5558;  
Sakai T and Okamoto K 2002 *Phys. Rev. B* **65** 214403;  
Schulenburg J and Richter J 2002 *Phys. Rev. B* **65** 054420;  
Chen X Y, Jiang Q and Wu Y Z 2002 *Solid State Commun.* **121** 641
- [5] Bethe H A 1931 *Z. Phys.* **71** 205;  
Hulthén L 1938 *Ark. Mat. Astron. Phys.* **26A** 1;  
Orbach R 1958 *Phys. Rev.* **112** 309;  
des Cloizeaux J and Gaudin M 1966 *J. Math. Phys.* **7** 1384;  
Yang C N and Yang C P 1966 *Phys. Rev.* **150** 321;  
Yang C N and Yang C P 1966 *Phys. Rev.* **150** 327;  
Yang C N and Yang C P 1966 *Phys. Rev.* **151** 258;  
Majumdar C K and Ghosh D K 1969 *J. Math. Phys.* **10** 1388;  
Majumdar C K and Ghosh D K 1969 *J. Math. Phys.* **10** 1399;  
Majumdar C K 1970 *J. Phys. C: Solid St. Phys.* **3** 911;  
Kirillov A N and Reshetikhin N Yu 1987 *J. Phys. A: Math. Gen.* **20** 1565;  
Kirillov A N and Reshetikhin N Yu 1987 *J. Phys. A: Math. Gen.* **20** 1587;  
Parkinson J B 1989 *J. Phys.: Condens. Matter* **1** 6709;  
Long M W and Fehrenbacher R 1990 *J. Phys.: Condens. Matter* **2** 2787;  
Long M W and Siak S 1990 *J. Phys.: Condens. Matter* **2** 10321;  
de Vega H J and Woynarovich F 1990 *J. Phys. A: Math. Gen.* **23** 1613;  
Kubo K 1993 *Phys. Rev. B* **48** 10552
- [6] de Vega H J and Woynarovich F 1992 *J. Phys. A: Math. Gen.* **25** 4499;  
Martins M J 1993 *J. Phys. A: Math. Gen.* **26** 7301;

- Dörfel B D and Meissner St 1996 *J. Phys. A: Math. Gen.* **29** 1949;  
Dörfel B D and Meissner St 1996 *J. Phys. A: Math. Gen.* **29** 6471;  
Dörfel B D and Meissner St 1997 *J. Phys. A: Math. Gen.* **30** 1931;  
Dörfel B D and Meissner St 1998 *J. Phys. A: Math. Gen.* **31** 61;  
Dörfel B D and Meissner St 1999 *J. Phys. A: Math. Gen.* **32** 41
- [7] Yao H, Li J and Gong Ch D 2002 *Solid State Commun.* **121** 687
- [8] Syozi I 1972 *Phase Transition and Critical Phenomena* ed C Domb and M S Green Vol. 1 (New York:Academic Press)
- [9] Lavis D A and Bell G M 1999 *Statistical Mechanics of Lattice Systems* Vol. 1 (Berlin: Springer Verlag)
- [10] Strečka J and Jaščur M 2002, *Phys. Rev. B* **66** 174415;  
Jaščur M and Strečka J 2002 *Acta Electrotechnica et Informatica* **2** 71;  
Strečka J and Jaščur M 2002 *Phys. Stat. Sol. (b)* **233** R12
- [11] Strečka J and Jaščur M 2002 *Czech. J. Phys.* **52** A37
- [12] Affleck I, Kennedy T, Lieb E H and Tasaki H 1987 *Phys. Rev. Lett* **59** 799
- [13] Gleizes A and Verdauger M 1981 *J. Am. Chem. Soc.* **103** 7373;  
Verdauger M, Julve M, Michalowicz A and Kahn O 1983 *Inorg. Chem.* **22** 2624;  
Drillon M, Gianduzzo J C and Gorges R 1983 *Phys. Lett. A* **96** 413;  
Gleizes A and Verdauger M 1984 *J. Am. Chem. Soc.* **106** 3727;  
Verdauger M, Gleizes A, Renard J P and Seiden J 1984 *Phys. Rev. B* **29** 5144;  
Gorges R, Drillon M and Currely J 1985 *J. Appl. Phys.* **58** 914;  
Kahn O 1987 *Struct. Bonding* (Berlin) **68** 91;  
Pei Y, Verdauger M, Kahn O, Sletten J and Renard J P 1987 *Inorg. Chem.* **26** 138;  
Kahn O, Pei Y, Verdauger M, Renard J P and Sletten J 1988 *J. Am. Chem. Soc.* **110** 782;  
Pei Y, Kahn O, Sletten J, Renard J P, Georges R, Gianduzzo J C, Currely J and Xu Q 1988 *Inorg. Chem.* **27** 47;  
Caneschi A, Gatteschi D, Renard J P, Rey P and Sessoli R 1989 *Inorg. Chem.* **28** 1976;  
Van Koningsbruggen P J, Kahn O, Nakatani K, Pei Y, Renard J P, Drillon M and Leggol P 1990 *Inorg. Chem.* **29** 3325;  
Kahn O, Pei Y and Journaux Y 1995 *Inorganic Materials* ed D W Bruce and D O'Hare (New York:Wiley);  
Hagiwara M, Minami K, Narumi Y, Tatani K and Kindo K 1998 *J. Phys. Soc. Jpn.* **67** 2209
- [14] Willet R D, Wang Z, Molnar S, Brewer K, Landee C P, Turnbull M M and Zhang W 1993 *Mol. Cryst. Liq. Cryst.* **233** 277;  
Kahn O 1993 *Molecular Magnetism* (New York:Verlag);  
Verdauger M 2001 *Polyhedron* **20** 1115;

- Černák J, Orendáč M, Potočňák I, Chomič J, Orendáčová A, Skoršepa J and Feher A 2002 *Coord. Chem. Rev.* **224** 51
- [15] Mukherjee P S, Maji T K, Mallah T, Zangrando E, Randaccio L and Chaudhuri N R 2001 *Inorg. Chim. Acta* **315** 249

## Figure captions

- Fig.1 Part of the doubly decorated mixed-spin chain. The black circles denote the spin-1/2 Ising atoms of sublattice  $A$  and the gray ones represent the decorating spin- $S$  Heisenberg atoms of sublattice  $B$ . The ellipse demarcates a typical bond described by the Hamiltonian  $\hat{\mathcal{H}}_k$  introduced in Eq. (2).
- Fig.2 Ground-state phase boundaries in the  $\Delta - H/J$  plane for  $J_1/J = 1.0$  and  $2.0$ .
- Fig.3 Low-temperature ( $k_B T/J = 0.01$ ) magnetization curves for: a)  $J_1/J = 1.0$  and  $\Delta = 1.0$ ; b)-d)  $J_1/J = 2.0$  and  $\Delta = 0.5, 1.0, 1.5$ . The solid and dotted (dashed) lines represent the total magnetization per one site and the single-site magnetization of the Ising (Heisenberg) sublattice, respectively.
- Fig.4 Low-temperature behaviour ( $k_B T/J = 0.01$ ) of several correlation functions:  $q_{hh}^{zz}$  and  $q_{ii}^{zz}$  (dashed lines),  $q_{hh}^{xx}$  (dotted lines) and  $q_{ih}^{zz}$  (solid lines).  
a) plot of the correlation functions against the anisotropy  $\Delta$  for the system without external field;  
b)-d) field-dependence of the correlation functions depicted for  $J_1/J = 2.0$  and various anisotropies  $\Delta = 0.5, 1.0$  and  $1.5$ .
- Fig.5 Thermal variations of the total magnetization for some typical values of the external field,  $J_1/J = 2.0$  and two selected anisotropies  $\Delta = 0.5$  and  $1.5$ , respectively.
- Fig.6 Thermal behaviour of the system for  $J_1/J = 2.0$ ,  $\Delta = 1.5$  and several values of external field.  
a) entropy plot versus temperature;  
b)-d) variations of the specific heat with temperature.
- Fig.7 Ground-state phase diagram together with some typical examples of low-temperature magnetization curves when the ratio  $J_1/J = 1.0$ ;  
a) ground-state phase diagram in the  $\Delta - H/J$  plane;  
b)-d) some typical examples of the low-temperature ( $k_B T/J = 0.001$ ) magnetization curves for various anisotropies  $\Delta$ .
- Fig.8 Low-temperature ( $k_B T/J = 0.001$ ) behaviour of several correlation functions  $q_{hh}^{zz}$  (dashed),  $q_{hh}^{xx}$  (dotted),  $q_{ih}^{zz}$  (solid),  $q_{ii}^{zz}$  (dashed-dotted), quadrupolar momentum  $\eta$  (dashed-dotted-dotted) and staggered sublattice magnetization  $m_B^s$  (solid line).  
a) zero-field variations of relevant quantities with anisotropy  $\Delta$ ;  
b)-d) field-dependencies of correlations for selected values of  $\Delta$ .
- Fig.9 Ground-state phase diagrams together with some typical examples of low-temperature magnetization curves:  
a)-b) ground-state phase diagram in the  $\Delta - H/J$  plane for  $J_1/J = 0.5$  and  $2.0$ ;  
c)-d) some typical examples of the low-temperature ( $k_B T/J = 0.001$ ) magnetization curves when  $J_1/J = 2.0$  and  $\Delta = 1.9$  and  $2.05$ , respectively.
- Fig.10 Thermal variations of the total magnetization for  $J_1/J = 1.0$  and two selected values of  $\Delta$ .



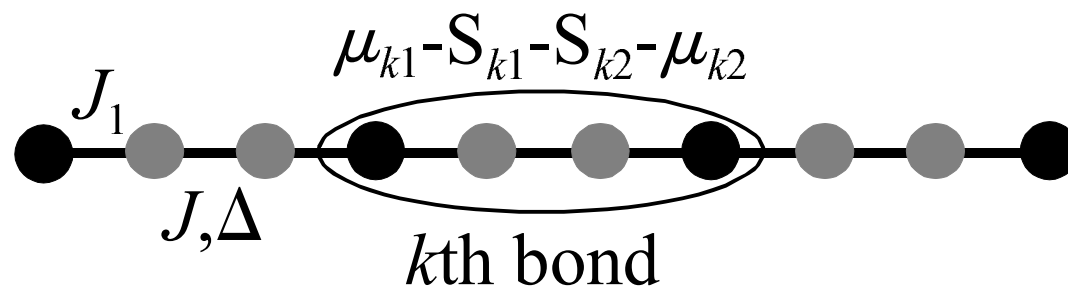


Fig.1 Strecka et al

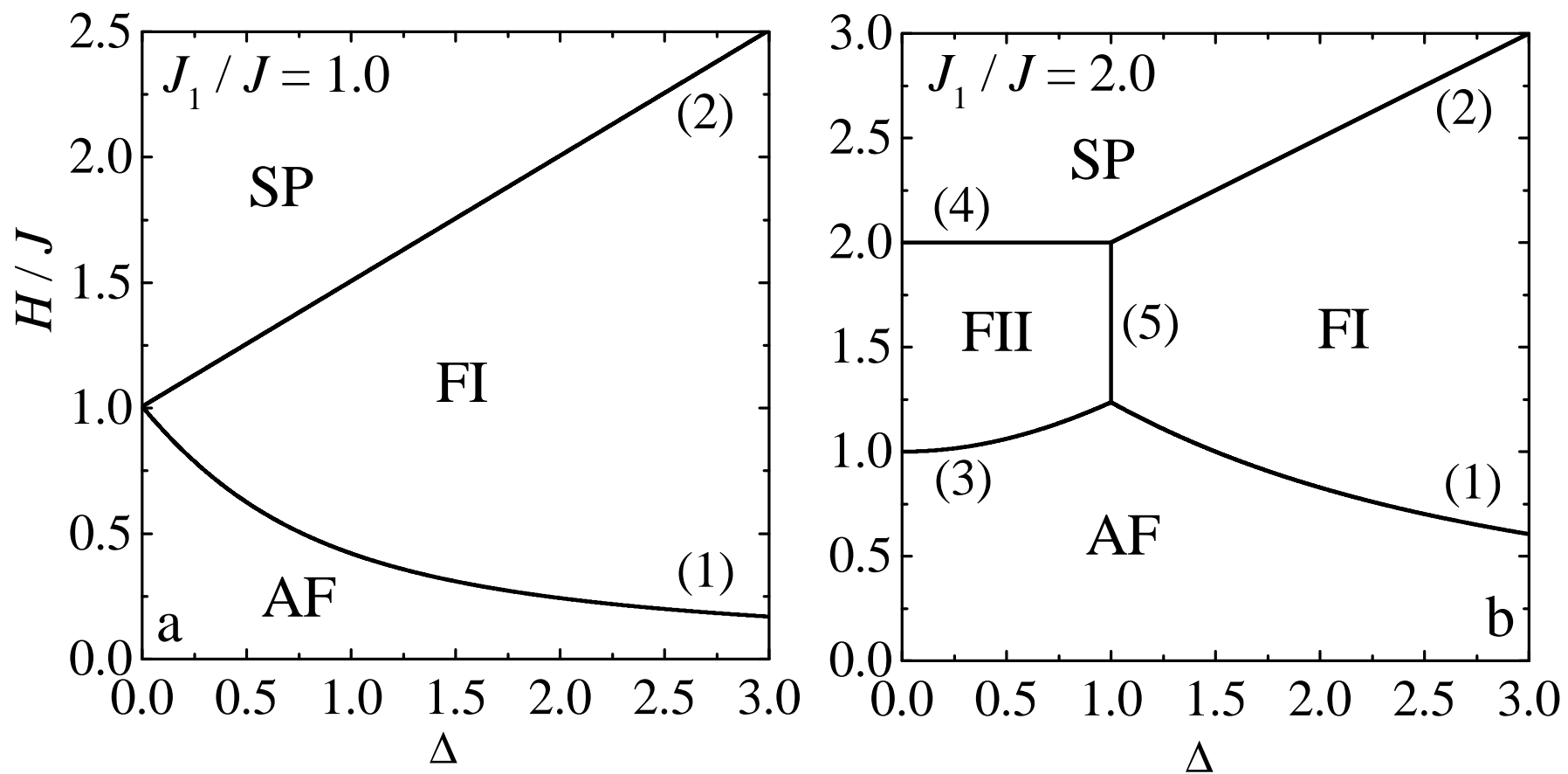


Fig.2 Strecka et al

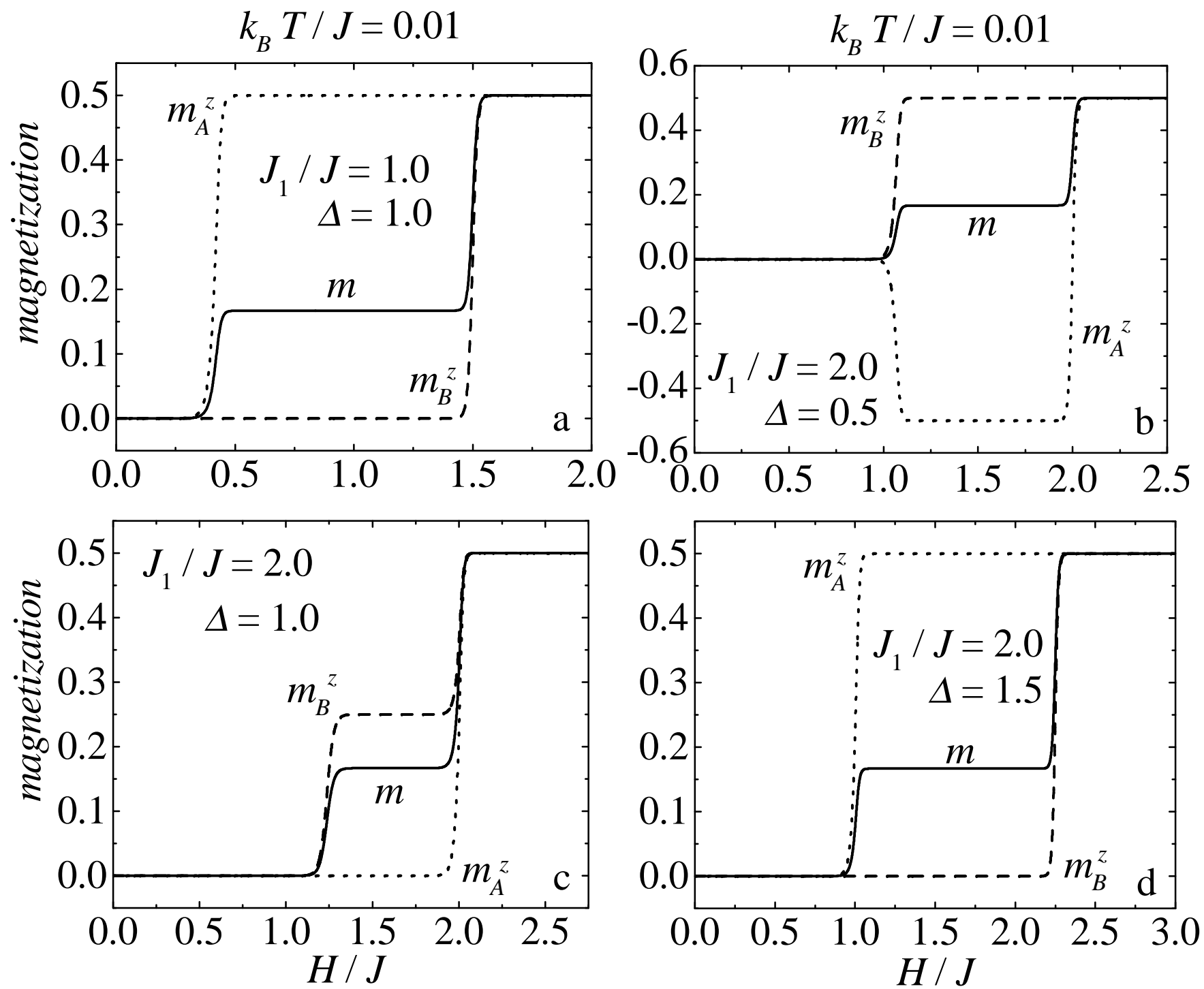


Fig. 3 Strecka et al

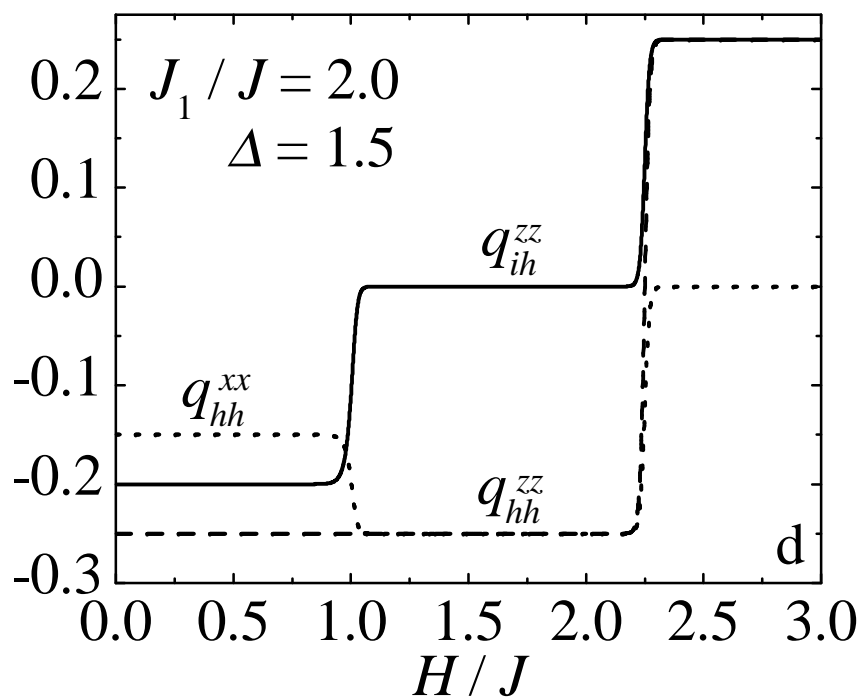
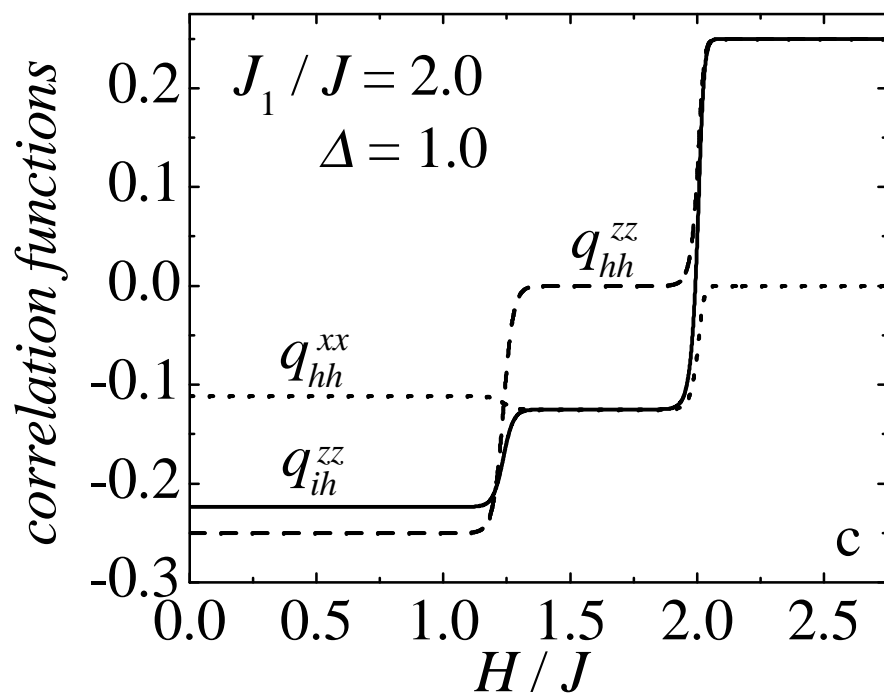
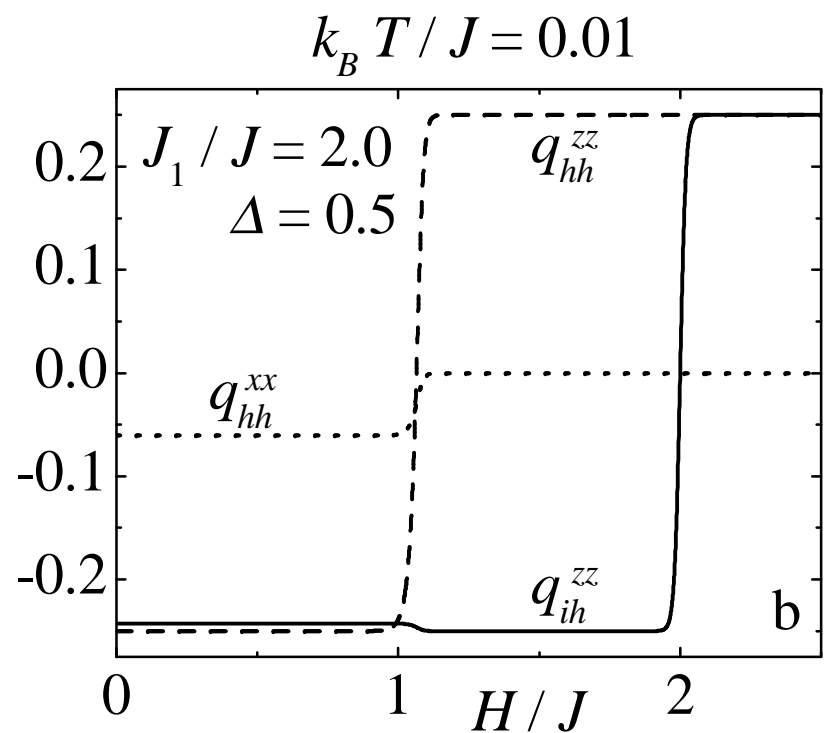
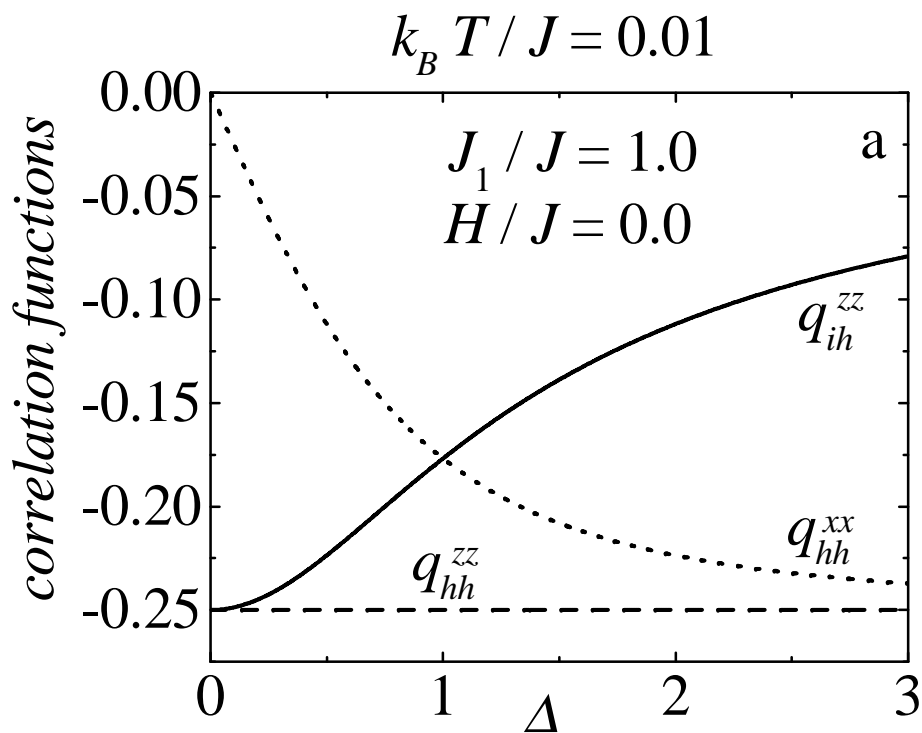


Fig. 4 Strecka et al

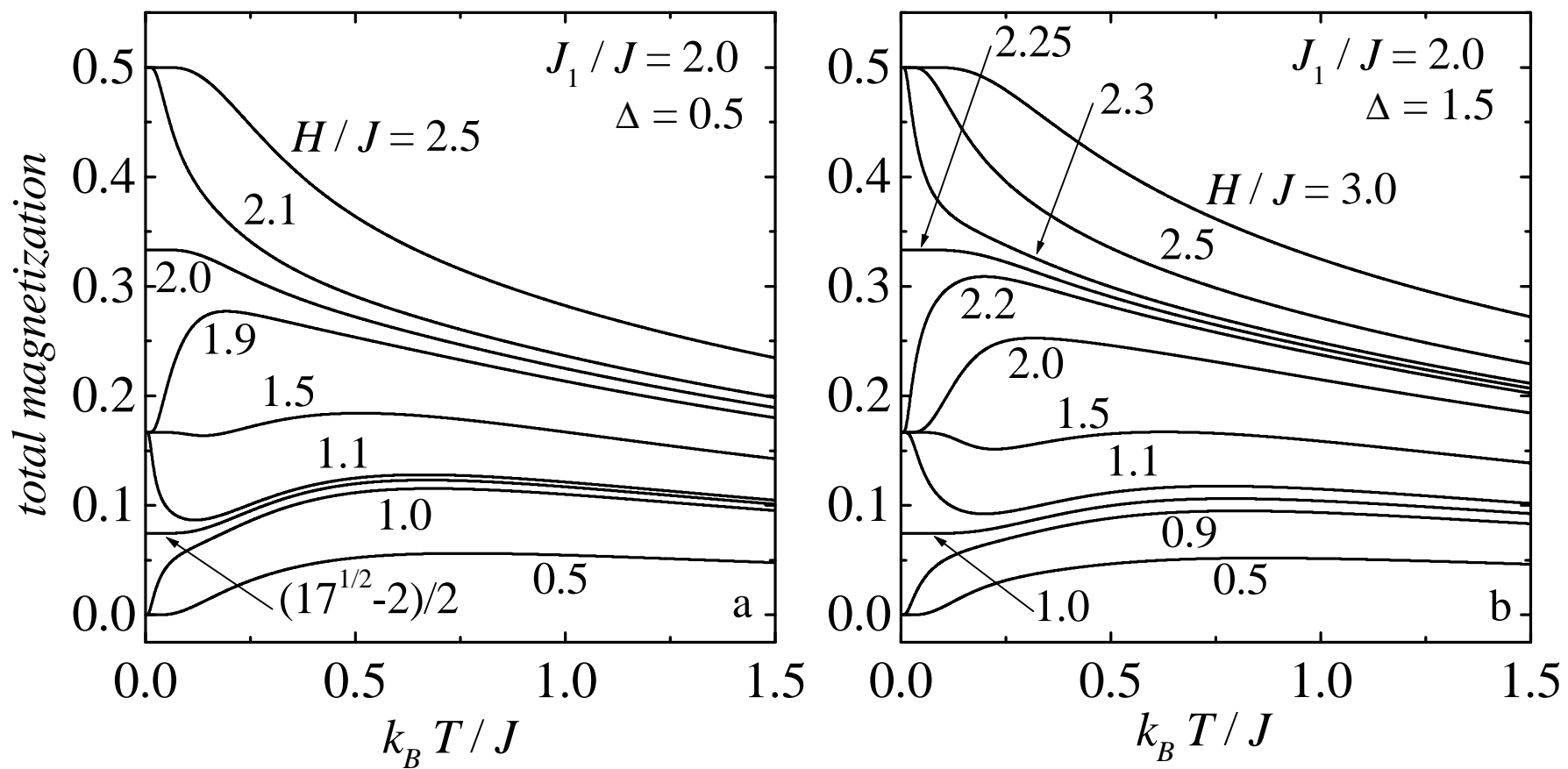


Fig.5 Strecka et al

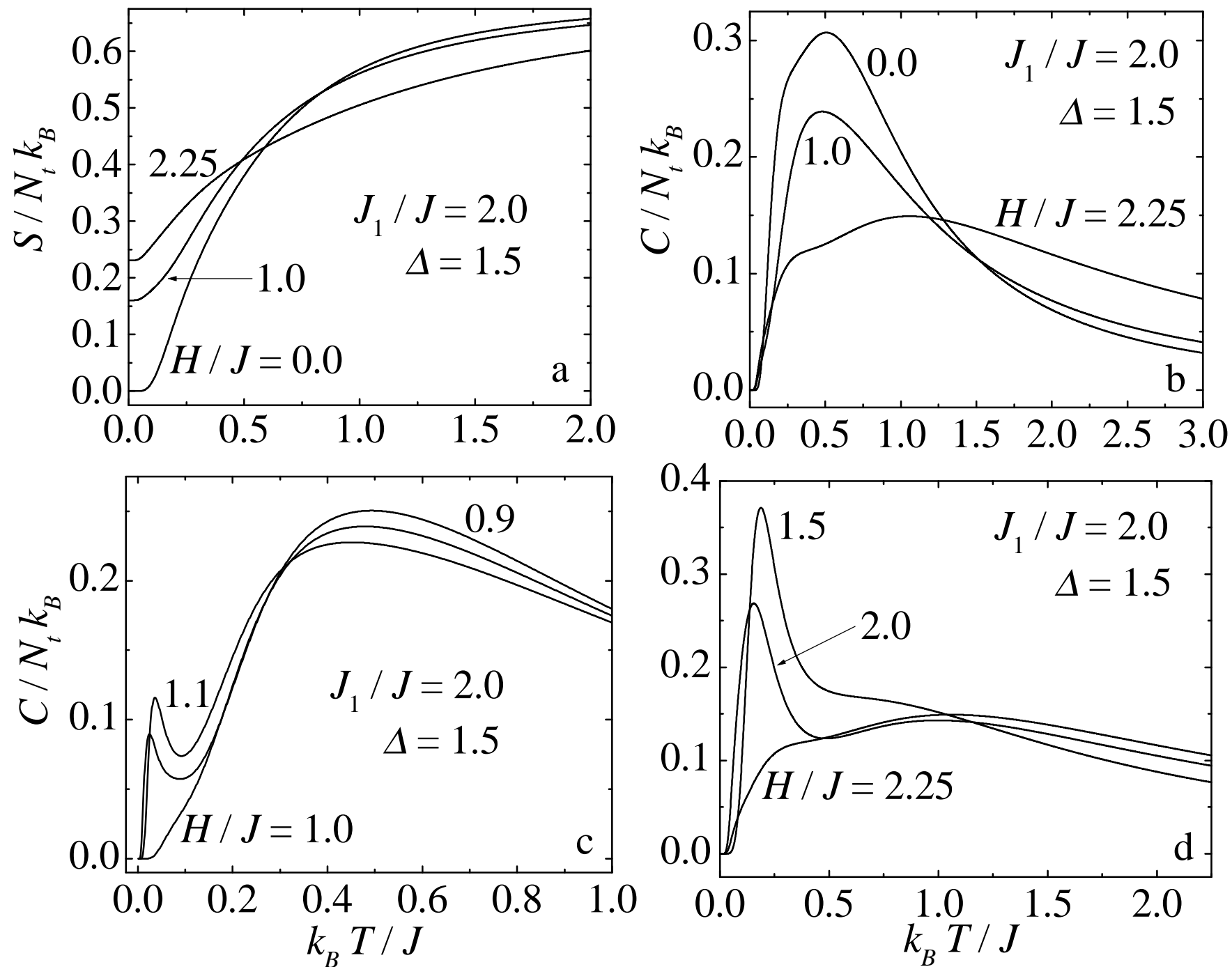


Fig. 6 Strecka et al

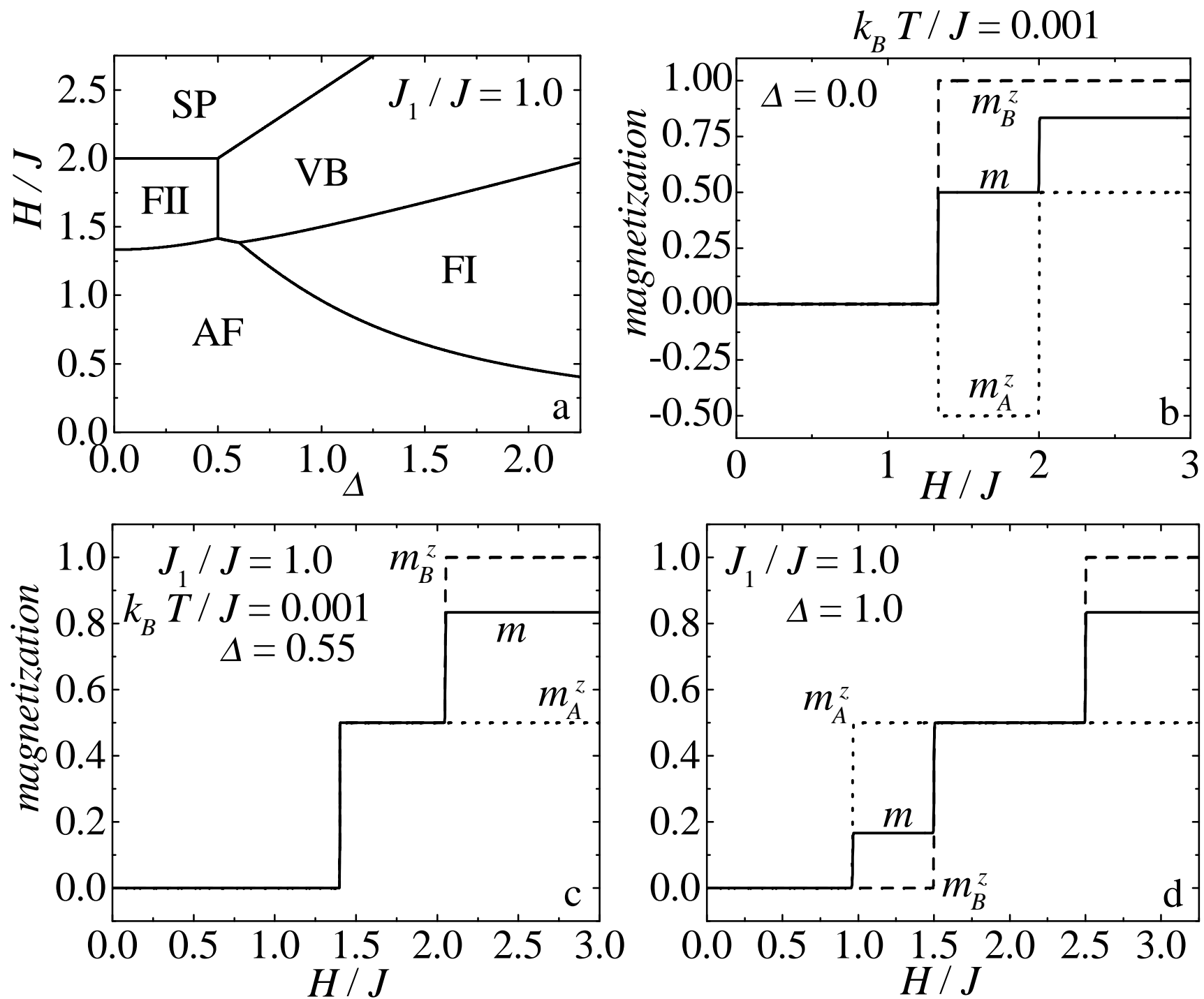


Fig.7 Strecka et al

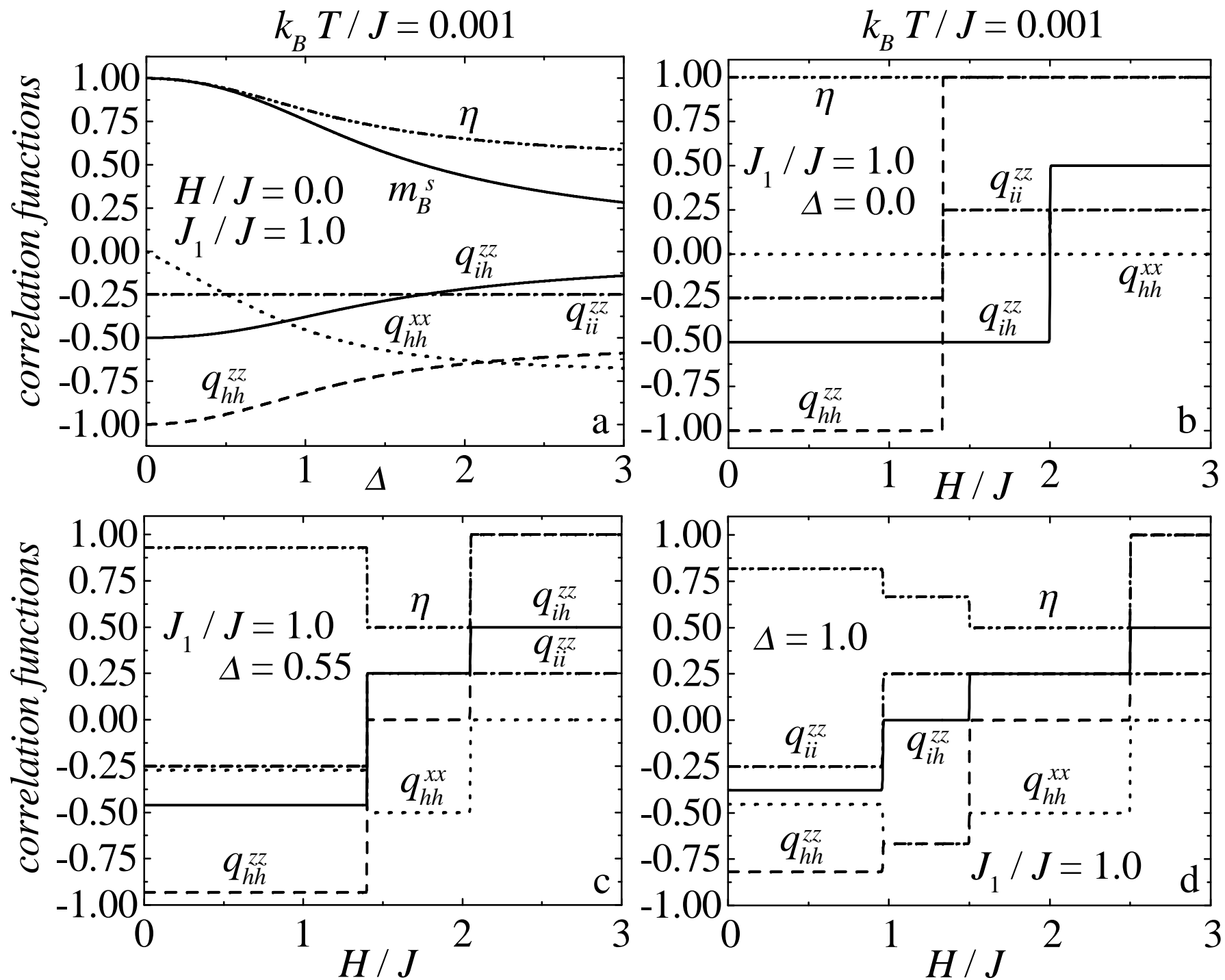


Fig 8 Strecka et al



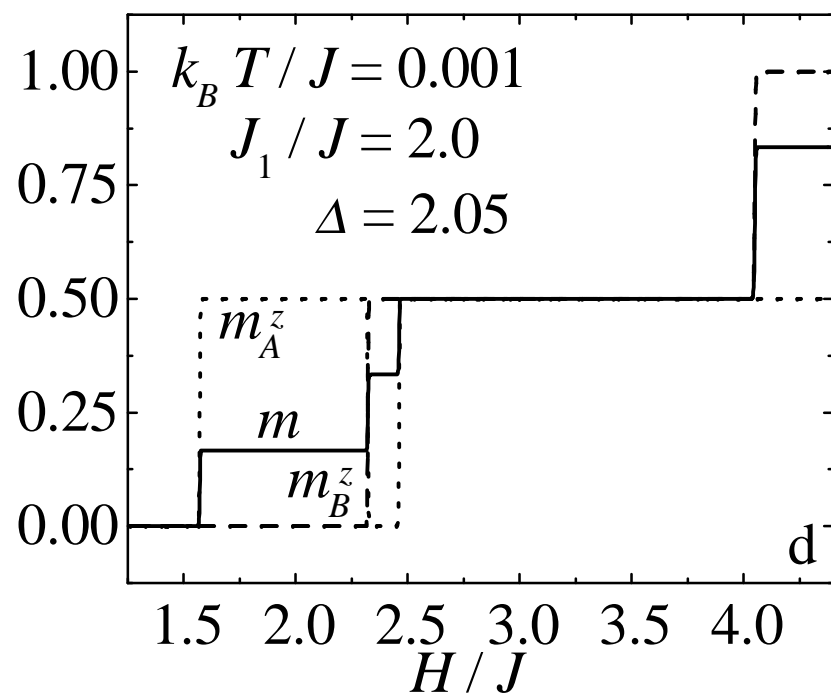
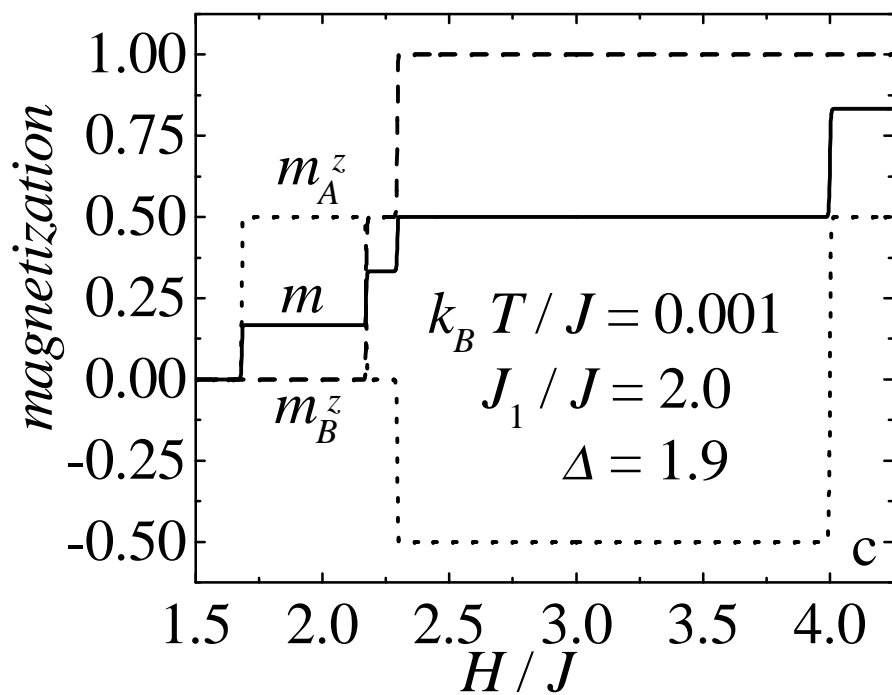
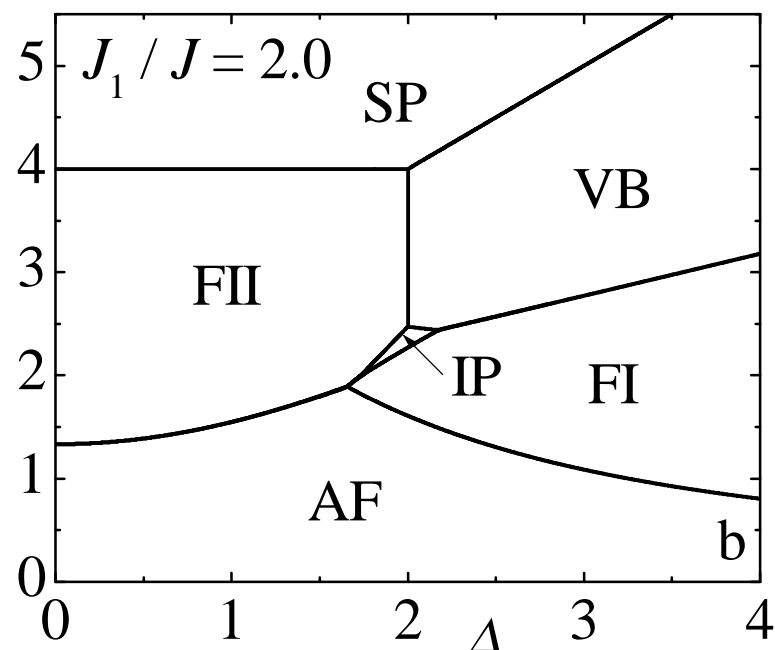
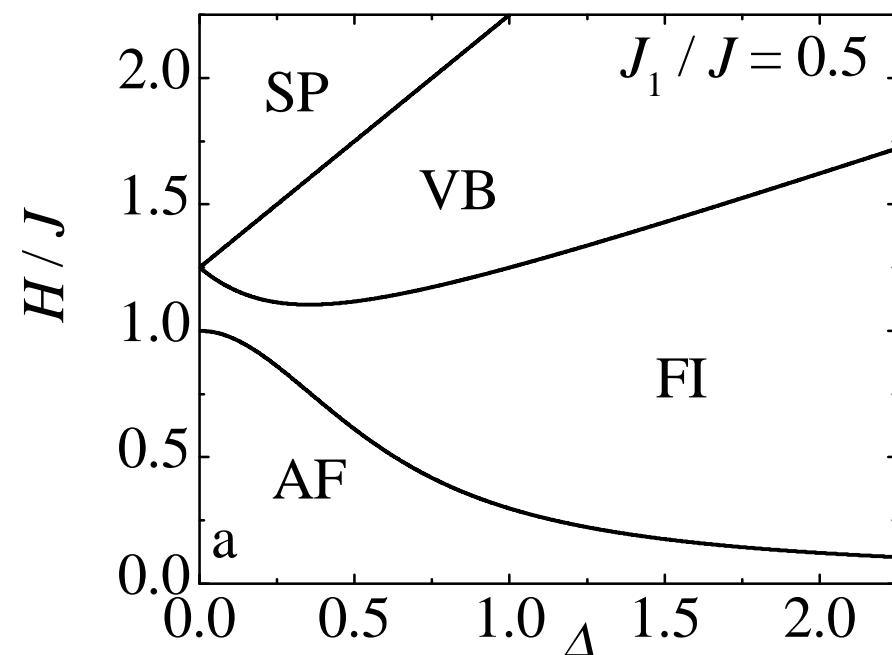


Fig. 9 Strecka et al.

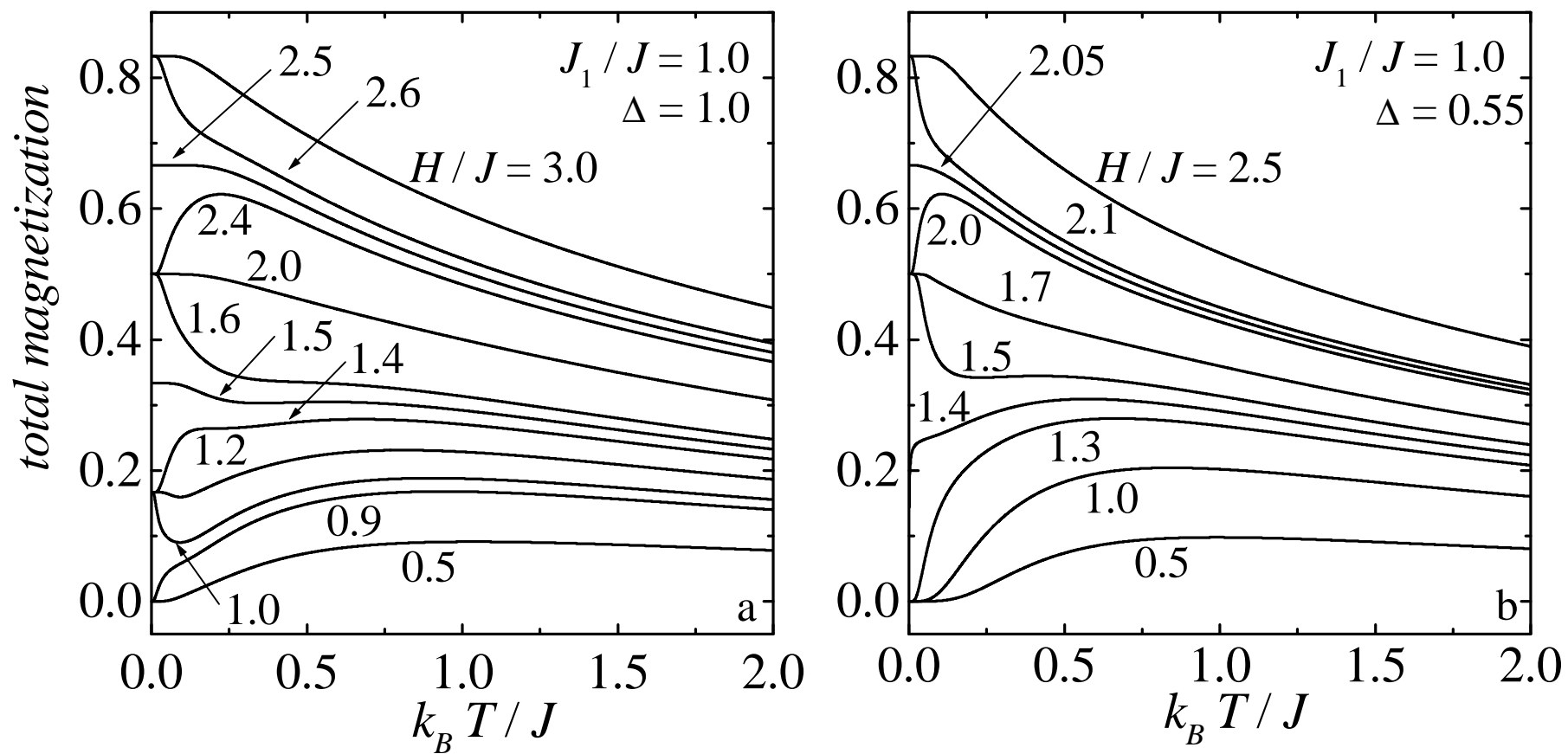


Fig.10 Strecka et al